Dentomaxillofacial Radiology (2016) 45, 20150281

birpublications.org/dmfr

RESEARCH ARTICLE

Ex vivo evaluation of new 2D and 3D dental radiographic technology for detecting caries

[1]Laurence Gaalaas, [2]Donald Tyndall, [2]André Mol, [3]Eric T Everett and [4]Ananta Bangdiwala

[1]Diagnostic and Biological Sciences, University of Minnesota School of Dentistry, Minneapolis, MN, USA; [2]Diagnostic Sciences, School of Dentistry, UNC Chapel Hill, Diagnostic Sciences, Chapel Hill, NC, USA; [3]Pediatric Dentistry, Dental Research, School of Dentistry, UNC Chapel Hill, Chapel Hill, NC, USA; [4]Biostatistics, McGavran-Greenberg Hall, Gillings School of Global Public Health, UNC Chapel Hill, Biostatistics, Chapel Hill, NC, USA

Objectives: Proximal dental caries remains a prevalent disease with only modest detection rates by current diagnostic systems. Many new systems are available without controlled validation of diagnostic efficacy. The objective of this study was to evaluate the diagnostic efficacy of three potentially promising new imaging systems.
Methods: This study evaluated the caries detection efficacy of Schick 33 (Sirona Dental, Salzburg, Austria) intraoral digital detector images employing an advanced sharpening filter, Planmeca ProMax® (Planmeca Inc., Helsinki, Finland) extraoral "panoramic bitewing" images and Sirona Orthophos XG3D (Sirona Dental) CBCT images with advanced artefact reduction. Conventional photostimulable phosphor images served as the control modality. An *ex vivo* study design using extracted human teeth, ten expert observers and micro-CT ground truth was employed.
Results: Receiver operating characteristic analysis indicated similar diagnostic efficacy of all systems (ANOVA $p > 0.05$). The sensitivity of the Schick 33 images (0.48) was significantly lower than the other modalities (0.53–0.62). The specificity of the Planmeca images (0.86) was significantly lower than Schick 33 (0.96) and XG3D (0.97). The XG3D showed significantly better cavitation detection sensitivity (0.62) than the other modalities (0.48–0.57).
Conclusions: The Schick 33 images demonstrated reduced caries sensitivity, whereas the Planmeca panoramic bitewing images demonstrated reduced specificity. XG3D with artefact reduction demonstrated elevated sensitivity and specificity for caries detection, improved depth accuracy and substantially improved cavitation detection. Care must be taken to recognize potential false-positive caries lesions with Planmeca panoramic bitewing images. Use of CBCT for caries detection must be carefully balanced with the presence of metal artefacts, time commitment, financial cost and radiation dose.
Dentomaxillofacial Radiology (2016) **45**, 20150281. doi: 10.1259/dmfr.20150281

Cite this article as: Gaalaas L, Tyndall D, Mol A, Everett ET, Bangdiwala A. *Ex vivo* evaluation of new 2D and 3D dental radiographic technology for detecting caries. *Dentomaxillofac Radiol* 2016; **45**: 20150281.

Keywords: dental caries; radiography, dental; bitewing radiography; cone-beam CT; MicroCT

Introduction

The radiographic detection rate of proximal caries is far from ideal as standard bitewing radiographs detect only about 60% of proximal lesions.[1–3] The relatively recent introduction of digital dental radiographic imaging has so far failed to demonstrate any increase in caries detection rates.[4–11] Overall, there does not yet appear to be an image enhancement algorithm that delivers clear gains in caries diagnosis.[12]

Compared with intraoral imaging, extraoral imaging using panoramic X-ray units promises improved patient

Correspondence to: Laurence Gaalaas. E-mail: gaal0017@umn.edu

The imaging core is supported in part by an NCI cancer centre Grant #P30-CA016086-35-37.
Received 28 August 2015; revised 9 December 2015; accepted 14 December 2015

comfort and efficiency. These modalities have been evaluated for their caries detection potential with mostly inferior performance compared with intraoral imaging owing to superimposition of additional structures, increased image blurriness and inconsistent opening of posterior proximal contacts.[13–15] At this time, the authors are aware of only one published study that has evaluated panoramic bitewing images (Planmeca Promax®; Planmeca Inc., Helsinki, Finland) for proximal caries detection, which found inferior detection rates compared with standard intraoral bitewing radiography.[16]

Many studies show that CBCT caries detection rates are approximately equivalent to intraoral modalities for non-restored teeth.[11,17–23] A recent review of the literature summarises that CBCT is equivalent to intraoral techniques at detecting clinically relevant caries lesions in minimally restored teeth; however, beam-hardening and streak artefacts from metal objects and dense tooth structure (enamel) are limiting factors.[24,25] Furthermore, increased dose, cost, time and artefact concerns dictate that bitewing radiographs are still the preferred modality for proximal caries detection.[26]

Broadly, caries diagnosis is not limited to simple lesion detection. Our understanding of the caries disease process has identified lesion depth, activity and cavitation status as significant indicators for the likelihood of lesion progression.[27,28] Assessment of lesion cavitation is also important because cavitated lesions demonstrate a much higher likelihood of progression.[28–30] Ultimately, the approach to identifying and treating incipient and early caries lesions non-restoratively places a maximum demand on radiographic imaging systems.[31–33] With regard to lesion detection, dentistry needs increased sensitivity from new diagnostic systems with no corresponding compromise in the already high specificity rates. Dentistry also needs improved ability to accurately identify lesion depth and lesion cavitation.[34]

A variety of dental imaging technologies have been recently introduced, each having developments that may increase caries detection. These new technologies include the Schick 33 (Schick 33) intraoral direct digital sensor (Sirona Dental, Salzburg, Austria), the Planmeca ProMax® (PanBW) panoramic unit in panoramic bitewing mode (Planmeca Inc.) and the Sirona Orthophos XG3D CBCT (XG3D) in high definition (HD) mode with metal artefact reduction software (MARS) (Sirona Dental).

The National Institutes of Health has called for continued research on diagnostic methods, including new devices and techniques.[31] All three of these imaging systems are available, yet there has been limited evaluation of their caries diagnostic performance. Accordingly, the aim of this project was to establish the diagnostic efficacy of these three new dental radiographic imaging technologies for assessing the presence, depth and cavitation status of proximal caries in non-restored teeth using an *ex vivo* study design.

Methods and materials

The Schick33 intraoral sensor has a dynamic image sharpening filter which may aid caries detection by improving lesion edge visualization.[35,36] PanBW images are acquired using the image projection geometry designed to open posterior dental contacts and consequently increase caries visibility. XG3D images with HD mode and MARS employ artefact reduction algorithms which may diminish beam-hardening and streak artefacts, both of which are limitations in CBCT caries imaging for restored as well as non-restored teeth.

Institutional review board approvals were obtained to collect deidentified extracted human teeth from existing specimen repositories and to perform observer sessions. Tooth selection criteria included premolar or molar teeth with an unrestored or minimally restored status with cervical (non-coronal, non-proximal) restoration involvement only. Selection criteria also included proximal caries status of sound/no-lesion or small-to-moderate-sized lesion as estimated by visual, tactile and bitewing radiographic means. Teeth with large, cavitated coronal lesions were excluded. A total of 29 extracted teeth were selected for the sample. 3 teeth were used twice giving a total sample size of 32 teeth (64 proximal surfaces). The three teeth were selected to be used twice because they demonstrated simultaneously classic proximal lesion morphology and challenging lesion visibility when screened with bitewing radiography. A power calculation for receiver operating characteristic (ROC) analysis provided an estimated sample size of 51 surfaces for this "paired-case, paired-reader" study design.[37–39]

A dry human mandible served as the *ex vivo* phantom for this study. Extracted teeth were held in residual extraction sockets with wax. Premolar–molar pairs were randomly selected from the sample to establish an anatomically appropriate pair of teeth for placement in the mandible. Non-restored and non-carious premolars and molars were placed anteriorly and posteriorly to the sample teeth. The mandible was restored bilaterally to best simulate the attenuation properties of scanning a normal dental arch. Efforts were made to make contacts as parallel as possible in order to minimize the confounding effect of closed contacts on the task of interpretation.

A 1-cm layer of dental "boxing" wax was placed around the mandible as a suitable simulation of soft-tissue attenuation. For the extraoral imaging modalities (XG3D and PanBW), an additional water balloon and a 3-mm thick aluminium cylinder with a 15.5-cm diameter were placed inside and around the mandible/wax phantom, respectively, to further simulate the attenuation properties of the human head relevant to extraoral imaging.

The control modality consisted of photostimulable phosphor (PSP) bitewing radiographs: Gendex Size 2 PSP plates (Gendex, Hatfield, PA) were exposed with

a Focus™ intraoral source (Instrumentarium Dental, Tuusula, Finland) at 70 kVp, 7 mA, 0.2 s and 40 cm source to image distance (SID) with standard rectangular collimation. The exposed plates were processed with a ScanX IO ILE scanner (Air Techniques, Melville, NY) through MiPACS Dental Enterprise Viewer 3.1 operating ScanX Plugin v. 1.2.8 (Medicore Imaging, Charlotte, NC). The Schick33 images were taken with the same Focus intraoral source at 70 kVp, 0.05 s and 40 cm SID standard rectangular collimation in the same manner as the PSP modality. The software interface for the Schick33 sensor was CDR DICOM for Windows® v. 4 (Sirona Dental). PanBW images were taken at 72 kVp and 11 mA with a square average jaw shape. The mandible was placed in the machine according to the standard anatomic positioning. Dexis v. 9.0.5 imaging software (Dexis LLC, Hatfield, PA) was used to acquire and store the images. XG3D scans were taken at 85 kVp and 6 mA with a 5 × 5-cm field of view (FOV) and 0.1-mm voxel size. Both HD mode and MARS were used. Scans were reconstructed and stored using Sidexis XG v. 2.56 software (Sirona Dental).

Caries ground truth status was established by micro-CT (microCT). The microCT scans were acquired with a SCANCO Medical μCT 40 scanner (Scanco Medical AG, Bruttisellen, Switzerland) operating at 70 kVp, 0.115 mA, 200-s scan time, with 0.5-mm aluminium filtration. Scans were reconstructed with a 20 μm voxel size using Scanco v. 1.2a software (SCANCO Medical AG). Teeth were scanned individually to avoid any pronounced beam-hardening artefacts due to adjacent teeth and/or restorations.

A total of 10 observers were recruited from the institution's Division of Oral and Maxillofacial Radiology. All observers had specialty-level training in oral and maxillofacial radiology and familiarity with diagnosing caries using intraoral, extraoral and three-dimensional imaging modalities. All observers participated in an orientation session prior to the interpretation sessions. The specific tasks asked of the observers for each proximal surface of each sample tooth were as follows. Task 1: rate the likelihood of caries presence on a 5-point scale where 1 = caries definitely not present, 2 = caries probably not present, 3 = unsure, 4 = caries probably present and 5 = caries definitely present. Task 2: rate the caries lesion depth on a 5-point scale where 1 = caries not present, 2 = caries involving the outer half of enamel, 3 = caries involving the inner half of enamel, 4 = caries involving the outer half of dentin and 5 = caries involving the inner half of dentin. Task 3: rate the likelihood of lesion cavitation on a 5-point scale where 1 = cavitation definitely not present, 2 = cavitation probably not present, 3 = unsure, 4 = cavitation probably present and 5 = cavitation definitely present. Observers used dual-monitor workstations with Lenovo LT2252P monitors (Lenovo, Beijing, China) as the primary diagnostic displays. All diagnostic displays passed TCG-18 test pattern quality control checks of the 5% and 95% contrast levels prior to the sessions. Ambient lighting in the room was subdued to appropriate interpretation levels.

MiPACS Dental Enterprise Viewer 3.1 (Medicore Imaging) was used as the PSP bitewing interpretation software. CDR DICOM for Windows® v. 5.4 was used for the Schick33 interpretation software. The general dentistry task with default 35% sharpening was selected for initial image display. DEXview v. 10.0.2 (Dexis LLC, Hatfield, PA) was used to view the panoramic bitewing images. Galaxis v. 1.9 (Sirona Dental) was used for the CBCT interpretation software. Observers were allowed to use brightness/contrast adjustment tools for their interpretation. Observers were also allowed to adjust the level of sharpening of the Schick33 images with the CDR software.

Following interpretation and discussion of the calibration set of images, the observers completed interpretation of images of all 32 subject teeth imaged by all four modalities. The sequence of image and modality interpretation was randomized so that no modality was biased towards the beginning or end of the session and no set of the same sample teeth were interpreted in succession. After a washout period of 2–3 weeks, observers returned to complete a second session. The observers interpreted images of exactly half of the subject teeth imaged by all four modalities (16 of 32).

To complete the caries ground truth analysis, each microCT scan was reviewed by the principal investigator and coauthor experienced with caries ground truth assessment to establish caries status, lesion depth and cavitation status of every proximal surface in the sample. Decision discrepancies were resolved by consensus following a discussion of the image findings.

ROC curves were constructed and fitted area-under-the-curve (A_Z) scores were recorded using a web-based ROC analysis tool (www.jrocfit.org). Caries presence detection and cavitation detection sensitivity and specificity scores were calculated for each observer–modality combination where caries presence ratings 4 and 5 were considered a positive diagnosis and caries ratings 1, 2 and 3 were considered a negative diagnosis. Observer–modality combination A_Z scores were compared with a fixed-effects main-effects two-way ANOVA. Sensitivity and specificity scores were compared with a fixed-effects Friedman's two-way non-parametric ANOVA using observer and modality as main factors. A non-parametric approach was chosen based on the non-normal behaviour of sensitivity and specificity scores. For both A_Z and sensitivity/specificity tests, a p-value <0.05 was considered statistically significant for overall test of effects. Wilcoxon rank-sum pairwise comparisons with Bonferroni adjustment were made when statistical significance was observed between modalities ($p < 0.05/6 = 0.0083$ was considered statistically significant).

Only true-positive observations were considered for depth accuracy analysis. For each observer's depth observation on each modality, the level of agreement between the depth observation and depth assessment by

microCT ground truth were calculated. Weighted kappa statistics were calculated using Cicchetti–Allison weights based on calculated scores. Weighted kappa coefficients for each modality were compared with one-way ANOVA. A p-value <0.05 was considered statistically significant for overall test of effects. *Post-hoc* t-test pairwise comparisons with Bonferroni adjustment were made when statistical significance was observed between modalities ($p < 0.05/6 = 0.0083$ was considered statistically significant).

The observation scores from the second session were used to determine the intraobserver agreement. For each of every observer's tooth surface assessment (presence, depth and cavitation), the level of agreement between the first and second session observations were calculated. It was assumed that images were independent and that ratings were independent. Weighted kappa statistics were calculated using Cicchetti–Allison weights based on scores. The median weighted kappa for each modality was determined, and coefficients for each observer were compared with one-way ANOVA. Analyses were performed using SAS® software v. 9.3 (SAS® Institute Inc., Cary, NC).

Results

Example images of extracted teeth and caries can be seen in Figure 1. A breakdown of proximal surface lesion status as determined by microCT is provided in Table 1. ROC curves for compiled caries presence observations by modality are provided in Figure 2. For the ROC analysis, fixed-effects main effects two-way ANOVA of A_Z scores indicated no significant difference between observers ($p = 0.15$) and between modalities ($p = 0.10$). Fixed-effects Friedman's two-way non-parametric ANOVA of caries presence sensitivity scores for the full data set indicated significant differences between observers ($p < 0.0001$) and between modalities ($p = 0.0002$). Similar analysis of specificity scores indicated significant differences between observers ($p = 0.0005$) and between modalities ($p = 0.0016$). Subsequent Wilcoxon rank-sum pairwise comparisons between modalities indicated that PSP (0.57) demonstrated a higher sensitivity than Schick33 (0.48) ($p = 0.0018$), XG3D demonstrated a higher sensitivity than Schick33 (0.48) ($p < 0.0001$) and XG3D (0.62) demonstrated a higher sensitivity than PanBW (0.53) ($p = 0.0071$).

Figure 1 Representative images of extracted teeth and caries for photostimulable phosphor (a), Schick 33 (Sirona Dental, Salzburg, Austria) (b), Planmeca panoramic bitewing (Planmeca Inc., Helsinki, Finland) (c), Sirona Orthophos XG3D CBCT (Sirona Dental) (d) and micro-CT ground truth (e). The lower right first molar is the same tooth in all images. Calibrations rods visualized in images are relevant to a separate study.

Table 1 Proximal surface ground truth status as assessed by micro-CT

Caries	*Surfaces*	*Depth*[a]	*Surfaces*	*Cavitation*	*Surfaces*
Sound	30	1	30	Absent	52
Lesion	34	2	9	Present	12
		3	9		
		4	14		
		5	2		
Total	64		64		64

[a]Lesion depth scale according to depth definitions in text.

Schick33 (0.96) demonstrated higher specificity than PanBW (0.86) ($p = 0.0005$) and XG3D (0.97) demonstrated a higher specificity than PanBW (0.86) ($p = 0.0013$).

The median accuracy of the observer-assigned depth scores were moderately high for PSP ($\kappa = 0.40$), Schick 33 ($\kappa = 0.43$) and XG3D, with XG3D having the best accuracy ($\kappa = 0.63$). The PanBW modality was considered fairly inaccurate ($\kappa = 0.27$). ANOVA of kappa coefficients indicated significant differences between modalities ($p = 0.003$). Pairwise comparisons indicated that XG3D had significantly better depth agreement than PanBW ($p = 0.002$).

For cavitation sensitivity scores, ANOVA indicated significant differences between observers ($p = 0.0063$) and between modalities ($p < 0.0001$). In cavitation specificity scores, there were similar significant differences between modalities ($p = 0.0025$) but no significant differences between observers ($p = 0.1829$). Pairwise comparisons indicated that XG3D (0.83) had higher sensitivity than PSP (0.54), Schick33 (0.47) and PanBW (0.38) ($p = 0.0011$, <0.0001 and <0.0001, respectively). XG3D (0.96) had statistically significant lower specificity than PSP (0.99) and Schick33 (0.99).

Overall, based on median weighted kappa, intraobserver agreement of caries presence was moderately high for each modality. Intraobserver agreement for caries depth was also moderately high for each modality. Intraobserver agreement of caries cavitation was moderately high as well for each modality. One-way ANOVA of kappa coefficients indicated no significant differences between modalities for caries presence, depth and cavitation ratings ($p = 0.411$, 0.376, 0.197, respectively). A summary of all statistical findings is provided in Table 2.

Discussion

ROC analysis was chosen because it removes the effect of observers' different diagnosis decision-making and provides the best overall indication of diagnostic accuracy to be compared between modalities.[40–42] ROC analysis of caries diagnosis indicated no significant differences between modalities' in terms of their A_Z scores. This suggests that all four modalities performed equally with respect to identifying lesions. One key nuance of ROC analysis, however, is that two separate ROC curves may have the exact same A_Z but different curve shapes, depending on the trade-off between sensitivity and specificity. This trade-off does not affect the overall diagnostic accuracy indication, but it is clinically relevant since it is much more beneficial to the patient and provider to maximize specificity because a false-positive lesion can result in unnecessary surgical treatment of the tooth at additional cost to the patient and significant detriment to the tooth's future restorative prognosis.[1] To reconcile these points with our previously stated desires for increased sensitivity, the authors reiterate that we desire improved sensitivity from new diagnostic systems with no corresponding penalty in the already high specificities.

Subsequent analysis of modality sensitivity and specificity scores elucidated potentially relevant clinical differences in performance. PSP (0.57) demonstrated a higher sensitivity than Schick33 (0.48), XG3D demonstrated a higher sensitivity than Schick33 (0.48) and XG3D (0.62) demonstrated a higher sensitivity than PanBW (0.53). Schick33 (0.96) demonstrated higher specificity than PanBW (0.86) and XG3D (0.97) demonstrated a higher specificity than PanBW (0.86). Finding significant differences between observers in the caries and cavitation sensitivity/specificity analyses was not surprising because these measures of diagnostic accuracy are dependent on the individual observer's decision threshold; therefore the specific ANOVA analyses for sensitivity/specificity results were chosen because they address observer variation before making a determination of significant modality effects.

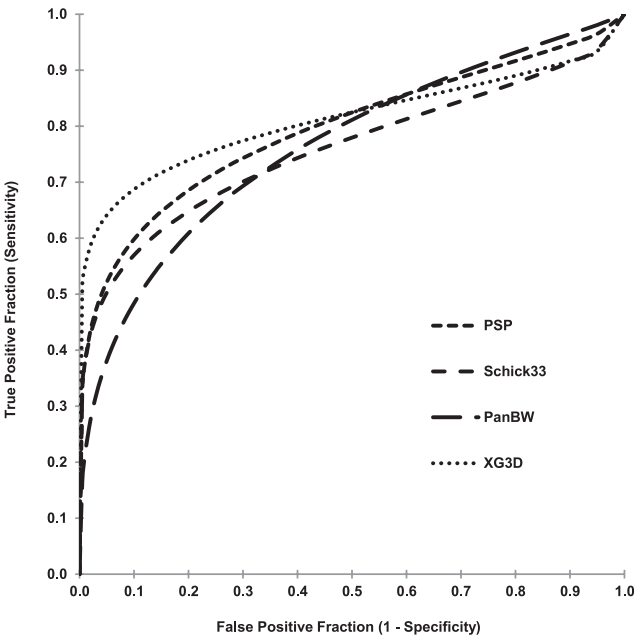

Figure 2 Receiver operating characteristic curves for each modality's compiled observations. PanBW from Planmeca Inc., Helsinki, Finland; PSP from Gendex, Hatfield, PA; and Schick33 and XG3D have been obtained from Sirona Dental, Salzburg, Austria.

Table 2 Summary of statistical findings comparing caries presence A_Z, caries sensitivity/specificity, depth observation weighted kappa correlation, cavitation sensitivity/specificity and intraobserver agreement

Data set, modality	*Diagnostic measure*	*Test effect*	p-*value*	*Pairwise comparison*	p-*value*
A_Z scores[a]	Mean $A_Z \pm 95\%$ CI				
PSP	0.820 ± 0.037				
Schick33	0.780 ± 0.032				
PanBW	0.791 ± 0.035				
XG3D	0.828 ± 0.020				
		Observer	0.15	N/A	N/A
		Modality	0.10	N/A	N/A
Caries sensitivity[b]	Mean sensitivity ± 95% CI				
PSP	0.57 ± 0.07				
Schick33	0.48 ± 0.09				
PanBW	0.53 ± 0.08				
XG3D	0.62 ± 0.07				
		Observer	<0.0001[c]		
		Modality	0.0002[c]		
				PSP *vs* PanBW	0.23
				PSP *vs* Schick33	0.0018[c]
				PSP *vs* XG3D	0.10
				PanBW *vs* Schick33	0.033
				PanBW *vs* XG3D	0.0071[c]
				Schick33 *vs* XG3D	<0.0001[c]
				Schick33 *vs* XG3D	0.73
Caries specificity[a]	Mean specificity ± 95% CI				
PSP	0.90 ± 0.08				
Schick33	0.96 ± 0.04				
PanBW	0.86 ± 0.09				
XG3D	0.97 ± 0.02				
		Observer	0.0005[c]		
		Modality	0.0016[c]		
				PSP *vs* PanBW	0.10
				PSP *vs* Shick33	0.034
				PSP *vs* XG3D	0.07
				PanBW *vs* Schick33	0.0005[c]
				PanBW *vs* XG3D	0.0013[c]
Lesion depth correlation with micro-CT (kappa)[d]	Median kappa (IQR)				
PSP	0.40 (0.30, 0.53)				
Schick33	0.43 (0.40, 0.50)				
PanBW	0.27 (0.23, 0.38)				
XG3D	0.63 (0.44, 0.72)				
		Modality	0.003[c]		
				PSP *vs* PanBW	0.62
				PSP *vs* Shick33	1.00
				PSP *vs* XG3D	0.15
				PanBW *vs* Schick33	0.32
				PanBW *vs* XG3D	0.002[c]
				Schick33 *vs* XG3D	0.30
Cavitation sensitivity[e]	Mean sensitivity ± 95% CI				
PSP	0.57 ± 0.14				
Schick33	0.48 ± 0.10				
PanBW	0.53 ± 0.11				
XG3D	0.62 ± 0.06				
		Observer	0.0063[c]		
		Modality	<0.0001[c]		
				PSP *vs* PanBW	0.043
				PSP *vs* Schick33	0.16
				PSP *vs* XG3D	0.0011[c]
				PanBW *vs* Schick33	0.50
				PanBW *vs* XG3D	<0.0001[c]
				Schick33 *vs* XG3D	<0.0001[c]
Cavitation specificity[e]	Mean specificity ± 95% CI				
PSP	0.90 ± 0.01				
Schick33	0.96 ± 0.01				
PanBW	0.86 ± 0.01				
XG3D	0.97 ± 0.02				
		Observer	0.18		
		Modality	0.0025[c]		

Table 2. Continued

Data set, modality	*Diagnostic measure*	*Test effect*	p-*value*	*Pairwise comparison*	p-*value*
				PSP *vs* PanBW	0.14
				PSP *vs* Schick33	0.78
				PSP *vs* XG3D	0.0015[c]
				PanBW *vs* Schick33	0.077
				PanBW *vs* XG3D	0.056
				Schick33 *vs* XG3D	0.0007[c]
Intraobserver agreement caries presence[f]	Median kappa (IQR)				
PSP	0.62 (0.57, 0.74)				
Schick33	0.73 (0.62, 0.81)				
PanBW	0.62 (0.52, 0.66)				
XG3D	0.65 (0.58, 0.74)				
		Modality	0.411	N/A	N/A
Intraobserver agreement caries depth[f]	Median kappa (IQR)				
PSP	0.76 (0.59, 0.81)				
Schick33	0.74 (0.66, 0.80)				
PanBW	0.66 (0.53, 0.740)				
XG3D	0.73 (0.70, 0.75)				
		Modality	0.376	N/A	N/A
Intraobserver agreement caries cavitation[f]	Median kappa (IQR)				
PSP	0.69 (0.60, 0.75)				
Schick33	0.70 (0.63, 0.81)				
PanBW	0.60 (0.41, 0.69)				
XG3D	0.72 (0.62, 0.80)				
		Modality	0.197	N/A	N/A

CI, confidence interval; IQR, interquartile range.
PanBW from Planmeca Inc., Helsinki, Finland; PSP from Gendex, Hatfield, PA; and Schick33 and XG3D have been obtained from Sirona Dental, Salzburg, Austria.
[a]Statistically significant difference.
[b]Fixed-effects main effects two-way ANOVA.
[c]Fixed-effects Friedman's two-way non-parametric ANOVA and Wilcoxon rank-sum pairwise comparison, Bonferroni adjustment ($p < 0.05$, $p < 0.0083$, respectively).
[d]One-way ANOVA with *t*-test pairwise comparison, Bonferroni adjustment ($p < 0.05$, $p < 0.0083$, respectively).
[e]Fixed-effects Friedman's two-way non-parametric ANOVA and Wilcoxon rank-sum pairwise comparison, Bonferroni adjustment ($p < 0.05$, $p < 0.0083$, respectively).
[f]One-way ANOVA.

The lower sensitivity of Schick33 may be attributable to the dynamic image-sharpening filter. Based on observer comments, it was found that different observers had different preferences for the level of sharpness. The immediate adjustment of image sharpness during interpretation may have distracted or otherwise influenced the observers into missing very subtle, difficult-to-detect lesions resulting in somewhat decreased sensitivity. Alternatively, the filter may have truly obscured lesions. However, this study did not test the influence of specific levels of image sharpening in the Schick33 system; therefore no definitive conclusions about the sharpening system itself can be made at this time.

Decreased specificity with the panoramic bitewing images may be attributable to image "ghost" artefacts from the contralateral aspect of the mandible formed as a result of image acquisition geometry, similar to that in traditional panoramic imaging.[13–15] Observers commented that horizontal tomographic streak artefacts from the contralateral body of the phantom mandible were superimposed over the teeth of interest, resulting in the perception that image interpretation was more challenging. It is possible that these artefacts may have mimicked lesions in a number of cases, resulting in an elevated false-positive rate. The authors are concerned that an elevated false-positive rate could have detrimental effects associated with caries treatment decisions.

The XG3D system demonstrated higher sensitivity than other modalities while maintaining high specificity. This finding is different than previous studies which cited beam-hardening artefacts from nearby enamel as a source of decreased specificity (increased false-positive diagnoses).[18,43] One possible explanation of reduced false-positive diagnoses is that the XG3D was operating in the HD mode with the MARS reconstruction algorithm. An alternative explanation is the investigators' demonstration of beam-hardening artefacts *vs* real caries lesions to the observers during orientation. This demonstration may have educated the observers to more consistently avoid false-positive diagnoses of artefacts as lesions much in the same way that well-trained dentists are able to differentiate caries from cervical burnout on two-dimensional images. Unfortunately, this study was designed to test the overall efficacy of the XG3D system compared with other modalities, therefore definitive conclusions cannot be drawn at this time. Regarding true-positive depth accuracy, the XG3D modality had significantly more accurate depth scores than the PanBW modality.

The XG3D system demonstrated an approximately 30% increase in detection of cavitated lesions compared

with other modalities. This finding is highly consistent with other recent studies. Our statistical analysis indicated that the XG3D (0.96) had significantly lower cavitation specificity than PSP (0.99) and Schick (0.99); however, these observed specificities are all extremely high. Therefore, it can be argued that the statistically significant cavitation specificity differences are clinically not relevant. Based on the findings in this study and other recent studies, it seems apparent that CBCT affords better detection of cavitated proximal lesions.[20,26,29]

Importantly, the authors reiterate that tooth selection criteria included premolar or molar teeth with an unrestored or minimally restored status with cervical (non-coronal, non-proximal) restoration involvement only. For these imaging systems, the effect of caries diagnosis on restored teeth on non-restored teeth with restorations within the scan FOV is undetermined at this time and warrants additional investigation. Also, the detrimental effect of patient motion on scan quality was not evaluated by this *ex vivo* study design and similarly warrants additional investigation.[44,45]

Finally, CBCT imaging incurs much greater radiation dose, financial cost and acquisition/interpretation time than other imaging modalities. The typical radiation dose for a CBCT scan varies widely from several micro Sieverts (μSv) to >1000 μSv, depending primarily on selected scan resolution and FOV.[46–48] The XG3D protocol used in this study had an effective dose of 53 μSv per mandibular posterior quadrant scan.[48] Comparatively, the dose from a standard set of four PSP or digital bitewing images is about 5 μSv, and dose from a standard panoramic image (approximately equal to a panoramic bitewing dose) is about 15 μSv.[46] The financial cost of CBCT imaging is significantly more than conventional bitewing or panoramic/panoramic bitewing examinations. The total acquisition and interpretation time for a CBCT is also significantly more than conventional bitewing or panoramic modalities. These costs must be carefully balanced with differences in diagnostic efficacy before selecting the imaging modality to address a relevant diagnostic question. With regard to caries detection, it is the authors' opinion that the marginal increase in lesion sensitivity, marginal increase in lesion depth assessment and even the substantial improvement in lesion cavitation detection may not be worth the significant increases in dose, cost and time. Of course, if a CBCT is taken for other clinical indications, it appears prudent to assess the visible regions of teeth for caries.

Almost all observer–modality combination weighted-kappa correlation scores were at least moderately agreeing ($\kappa > 0.40$). A review of similar multireader ROC studies cites a range of intraobserver agreement from 0.35 to 0.59,[49] confirming typical results in this study. No statistically significant differences in intraobserver agreement scores were observed between modalities for the caries presence, caries depth and caries cavitation questions. This finding indicates that our observers performed uniformly throughout the study without a modality effect.

A limitation of this study was the ideal conditions established for proximal caries diagnosis. These ideal conditions were chosen to best control confounding variables and isolate the actual differences in detection efficacy between modalities, but they may not represent clinically relevant interpretation scenarios. Interpretation took place under ideal viewing conditions with subdued ambient lighting, quiet surroundings and contrast calibrated monitors. Additionally, the observers were qualified experts in dental radiographic diagnosis, each having specialty training in oral and maxillofacial radiology and a detailed knowledge of radiographic caries diagnosis beyond the general dental level. Finally, all images were acquired with ideal image geometry resulting in open proximal contacts, whereas clinical imaging of real patients dictates that it is not always possible to open all posterior proximal contacts.

The traditional gold-standard method to validate dental caries status is microscopic examination of thin sections; however, in recent years, microCT has proven to be an effective alternative. Numerous studies have employed microCT as a ground truth caries validation tool for the purpose of caries detection.[39,50] MicroCT has also been shown to agree with transverse microradiography, another accepted gold-standard technique for the evaluation of caries.[51] The selection of 70 kVp tube potential and system calibration efforts in this study's microCT analysis are well supported by the literature.[52]

Conclusions

- This study found equivalent overall diagnostic efficacy for posterior proximal caries detection between three new and one control dental radiographic systems.
- The Schick 33 intraoral sensor demonstrated reduced caries sensitivity compared with other modalities.
- The Planmeca panoramic bitewing modality demonstrated an elevated false-positive rate with potentially clinically relevant implications for treatment decisions.
- The CBCT with artefact reduction demonstrated promising sensitivity/specificity for caries detection, somewhat improved depth accuracy and substantially improved cavitation detection.
- Practitioners must carefully balance caries detection on CBCT with the presence of metal artefacts, time commitment, financial cost and radiation dose.
- This study was performed with expert observers under ideal viewing conditions with ideal image geometry. These features of study design were chosen to best evaluate the diagnostic capabilities of the specific experimental modalities. Accordingly, the results may not apply to all clinical scenarios, environments and modalities. More research is needed to further clarify caries detection with modern imaging systems.

Acknowledgments

The authors thank Dr Thomas Schaaf for generously offering his time and access to the Planmeca unit; Dr John Preisser, Jr and Adane Wogu for their statistical support; Sirona Dental Inc. USA for their donation of a Schick33 intraoral sensor and imaging software; Dr Mansur Ahmad for his assistance with figure preparation; and the Small Animal Imaging Core facility at the UNC Biomedical Imaging Research Center for providing the micro-CT imaging service.

Conflicts of interest

The author Dr Donald Tyndall is a consultant for Sirona Dental Inc. This entity had no input into study design, collection/analysis/reporting of results or decision of publication.

References

1. Dove SB. Radiographic diagnosis of dental caries. *J Dent Educ* 2001; **65**: 985–90.
2. Douglass CW, Valachovic RW, Wijesinha A, Chauncey HH, Kapur KK, McNeil BJ. Clinical efficacy of dental radiography in the detection of dental caries and periodontal diseases. *Oral Surg Oral Med Oral Pathol* 1986; **62**: 330–9. doi: 10.1016/0030-4220(86)90017-4
3. Bader JD, Shugars DA, Bonito AJ. Systematic reviews of selected dental caries diagnostic and management methods. *J Dent Educ* 2001; **65**: 960–8.
4. White SC, Yoon DC. Comparative performance of digital and conventional images for detecting proximal surface caries. *Dentomaxillofac Radiol* 1997; **26**: 32–8. doi: 10.1038/sj.dmfr.4600208
5. Khan EA, Tyndall DA, Ludlow JB, Caplan D. Proximal caries detection: Sirona Sidexis *versus* Kodak Ektaspeed Plus. *Gen Dent* 2005; **53**: 43–8.
6. Wenzel A. Digital radiography and caries diagnosis. *Dentomaxillofac Radiol* 1998; **27**: 3–11. doi: 10.1038/sj.dmfr.4600321
7. Wenzel A. Bitewing and digital bitewing radiography for detection of caries lesions. *J Dental Res* 2004; **83**: C72–5. doi: 10.1177/154405910408301S14
8. Wenzel A. Digital imaging for dental caries. *Dent Clin North Am* 2000; **44**: 319–38.
9. Syriopoulos K, Sanderink GC, Velders XL, van der Stelt PF. Radiographic detection of approximal caries: a comparison of dental films and digital imaging systems. *Dentomaxillofac Radiol* 2000; **29**: 312–18. doi: 10.1038/sj.dmfr.4600553
10. Dove SB, McDavid WD. A comparison of conventional intraoral radiography and computer imaging techniques for the detection of proximal surface dental caries. *Dentomaxillofac Radiol* 1992; **21**: 127–34. doi: 10.1038/dmfr.21.3.1397467
11. Senel B, Kamburoglu K, Uçok O, Yüksel SP, Ozen T, Avsever H. Diagnostic accuracy of different imaging modalities in detection of proximal caries. *Dentomaxillofac Radiol* 2010; **39**: 501–11. doi: 10.1259/dmfr/28628723
12. Wenzel A. A review of dentists' use of digital radiography and caries diagnosis with digital systems. *Dentomaxillofac Radiol* 2006; **35**: 307–14. doi: 10.1259/dmfr/64693712
13. Akkaya N, Kansu O, Kansu H, Cagirankaya LB, Arslan U. Comparing the accuracy of panoramic and intraoral radiography in the diagnosis of proximal caries. *Dentomaxillofac Radiol* 2006; **35**: 170–4. doi: 10.1259/dmfr/26750940
14. Flint DJ, Paunovich E, Moore WS, Wofford DT, Hermesch CB. A diagnostic comparison of panoramic and intraoral radiographs. *Oral Surg Oral Med Oral Pathol Oral Radiol Endod* 1998; **85**: 731–5.
15. Akarslan ZZ, Akdevelioğlu M, Güngör K, Erten H. A comparison of the diagnostic accuracy of bitewing, periapical, unfiltered and filtered digital panoramic images for approximal caries detection in posterior teeth. *Dentomaxillofac Radiol* 2008; **37**: 458–63. doi: 10.1259/dmfr/84698143
16. Kamburoglu K, Kolsuz E, Murat S, Yüksel S, Ozen T. Proximal caries detection accuracy using intraoral bitewing radiography, extraoral bitewing radiography and panoramic radiography. *Dentomaxillofac Radiol* 2012; **41**: 450–9. doi: 10.1259/dmfr/30526171
17. Park YS, Ahn JS, Kwon HB, Lee SP. Current status of dental caries diagnosis using cone beam computed tomography. *Imaging Sci Dent* 2011; **41**: 43–51. doi: 10.5624/isd.2011.41.2.43
18. Rathore S, Tyndall D, Wright J, Everett E. *Ex vivo* comparison of Galileos cone beam CT and intraoral radiographs in detecting occlusal caries. *Dentomaxillofac Radiol* 2012; **41**: 489–93. doi: 10.1259/dmfr/57329547
19. Valizadeh S, Tavakkoli MA, Karimi Vasigh H, Azizi Z, Zarrabian T. Evaluation of cone beam computed tomography (CBCT) system: comparison with intraoral periapical radiography in proximal caries detection. *J Dent Res Dent Clin Dent Prospects* 2012; **6**: 1–5.
20. Wenzel A, Hirsch E, Christensen J, Matzen LH, Scaf G, Frydenberg M. Detection of cavitated approximal surfaces using cone beam CT and intraoral receptors. *Dentomaxillofac Radiol* 2013; **42**: 39458105. doi: 10.1259/dmfr/39458105
21. Tsuchida R, Araki K, Okano T. Evaluation of a limited cone-beam volumetric imaging system: comparison with film radiography in detecting incipient proximal caries. *Oral Surg Oral Med Oral Pathol Oral Radiol Endod* 2007; **104**: 412–16. doi: 10.1016/j.tripleo.2007.02.028
22. Kalathingal SM, Mol A, Tyndall DA, Caplan DJ. *In vitro* assessment of cone beam local computed tomography for proximal caries detection. *Oral Surg Oral Med Oral Pathol Oral Radiol Endod* 2007; **104**: 699–704. doi: 10.1016/j.tripleo.2006.08.032
23. Kayipmaz S, Sezgin ÖS, Saricaoğlu ST, Can G. An *in vitro* comparison of diagnostic abilities of conventional radiography, storage phosphor, and cone beam computed tomography to determine occlusal and approximal caries. *Eur J Radiol* 2011; **80**: 478–82. doi: 10.1016/j.ejrad.2010.09.011
24. Schulze R, Heil U, Gross D, Bruellmann DD, Dranischnikow E, Schwanecke U, et al. Artefacts in CBCT: a review. *Dentomaxillofac Radiol* 2011; **40**: 265–73. doi: 10.1259/dmfr/30642039
25. Draenert FG, Coppenrath E, Herzog P, Muller S, Mueller-Lisse UG. Beam hardening artefacts occur in dental implant scans with the NewTom cone beam CT but not with the dental 4-row multidetector CT. *Dentomaxillofac Radiol* 2007; **36**: 198–203. doi: 10.1259/dmfr/32579161
26. Wenzel A. Radiographic display of carious lesions and cavitation in approximal surfaces: advantages and drawbacks of conventional and advanced modalities. *Acta Odontol Scand* 2014; **72**: 251–64. doi: 10.3109/00016357.2014.888757
27. Baelum V. What is an appropriate caries diagnosis? *Acta Odontol Scand* 2010; **68**: 65–79. doi: 10.3109/00016350903530786
28. Kidd EA, Fejerskov O. What constitutes dental caries? Histopathology of carious enamel and dentin related to the action of cariogenic biofilms. *J Dent Res* 2004; **83**: C35–8.
29. Sansare K, Raghav M, Sontakke S, Karjodkar F, Wenzel A. Clinical cavitation and radiographic lesion depth in proximal surfaces in an Indian population. *Acta Odontol Scand* 2014; **72**: 1084–8. doi: 10.3109/00016357.2014.926025
30. Ferreira Zandoná A, Santiago E, Eckert GJ, Katz BP, Pereira de Oliveira S, Capin OR, et al. The natural history of dental caries lesions: a 4-year observational study. *J Dent Res* 2012; **91**: 841–6. doi: 10.1177/0022034512455030
31. Diagnosis and management of dental caries throughout life. National Institutes of Health Consensus Development Conference statement, March 26-28, 2001. *J Dent Educ* 2001; **65**: 1162–8.
32. Selwitz RH, Ismail AI, Pitts NB. Dental caries. *The Lancet* 2007; **369**: 51–9. doi: 10.1016/S0140-6736(07)60031-2

33. Braga MM, Mendes FM, Ekstrand KR. Detection activity assessment and diagnosis of dental caries lesions. *Dent Clin North Am* 2010; **54**: 479–93. doi: 10.1016/j.cden.2010.03.006
34. Wenzel A. Current trends in radiographic caries imaging. *Oral Surg Oral Med Oral Pathol Oral Radiol Endod* 1995; **80**: 527–39. doi: 10.1016/S1079-2104(05)80152-0
35. Kashima I. Computed radiography with photostimulable phosphor in oral and maxillofacial radiology. *Oral Surg Oral Med Oral Pathol Oral Radiol Endod* 1995; **80**: 577–98. doi: 10.1016/S1079-2104(05)80155-6
36. Huda W, Rill LN, Benn DK, Pettigrew JC. Comparison of a photostimulable phosphor system with film for dental radiology. *Oral Surg Oral Med Oral Pathol Oral Radiol Endod* 1997; **83**: 725–31. doi: 10.1016/S1079-2104(97)90327-9
37. Obuchowski NA. Multireader receiver operating characteristic studies: a comparison of study designs. *Acad Radiol* 1995; **2**: 709–16. doi: 10.1016/S1076-6332(05)80441-6
38. Obuchowski NA. How many observers are needed in clinical studies of medical imaging? *AJR Am J Roentgenol* 2004; **182**: 867–9. doi: 10.2214/ajr.182.4.1820867
39. Park YS, Bae KH, Chang J, Shon WJ. Theory of X-ray microcomputed tomography in dental research: application for the caries research. *J Korean Acad Conservative Dentistry* 2011; **36**: 98–107. doi: 10.5395/JKACD.2011.36.2.98
40. Metz CE. Basic principles of ROC analysis. *Semin Nucl Med* 1978; **8**: 283–98. doi: 10.1016/S0001-2998(78)80014-2
41. Metz CE. ROC methodology in radiologic imaging. *Invest Radiol* 1986; **21**: 720–33. doi: 10.1097/00004424-198609000-00009
42. ten Bosch JJ, Angmar-Månsson B. Characterization and validation of diagnostic methods. *Monogr Oral Sci* 2000; **17**: 174–89.
43. Tyndall DA, Rathore S. Cone-beam CT diagnostic applications: caries, periodontal bone assessment, and endodontic applications. *Dent Clin North Am* 2008; **52**: 825–41. doi: 10.1016/j.cden.2008.05.002
44. Hanzelka T, Dusek J, Ocasek F, Kucera J, Sedy J, Benes J, et al. Movement of the patient and the cone beam computed tomography scanner: objectives and possible solutions. *Oral Surg Oral Med Oral Pathol Oral Radiol* 2013; **116**: 769–73. doi: 10.1016/j.oooo.2013.08.010
45. Spin-Neto R, Mudrak J, Matzen LH, Christensen J, Gotfredsen E, Wenzel A. Cone beam CT image artefacts related to head motion simulated by a robot skull: visual characteristics and impact on image quality. *Dentomaxillofac Radiol* 2013; **42**: 32310645. doi: 10.1259/dmfr/32310645
46. Ludlow JB, Davies-Ludlow LE, White SC. Patient risk related to common dental radiographic examinations: the impact of 2007 International Commission on Radiological Protection recommendations regarding dose calculation. *J Am Dent Assoc* 2008; **139**: 1237–43. doi: 10.14219/jada.archive.2008.0339
47. Ludlow JB, Ivanovic M. Comparative dosimetry of dental CBCT devices and 64-slice CT for oral and maxillofacial radiology. *Oral Surg Oral Med Oral Pathol Oral Radiol Endod* 2008; **106**: 106–14. doi: 10.1016/j.tripleo.2008.03.018
48. Ludlow JB, Timothy R, Walker C, Hunter R, Benavides E, Samuelson DB, et al. Effective dose of dental CBCT-a meta analysis of published data and additional data for nine CBCT units. *Dentomaxillofac Radiol* 2015; **44**: 20140197. doi: 10.1259/dmfr.20140197
49. Rockette HE, Campbell WL, Britton CA, Holbert JM, King JL, Gur D. Empiric assessment of parameters that affect the design of multireader receiver operating characteristic studies. *Acad Radiol* 1999; **6**: 723–9. doi: 10.1016/S1076-6332(99)80468-1
50. Soviero VM, Leal SC, Silva RC, Azevedo RB. Validity of MicroCT for *in vitro* detection of proximal carious lesions in primary molars. *J Dent* 2012; **40**: 35–40. doi: 10.1016/j.jdent.2011.09.002
51. Hamba H, Nikaido T, Sadr A, Nakashima S, Tagami J. Enamel lesion parameter correlations between polychromatic micro-CT and TMR. *J Dent Res* 2012; **91**: 586–91. doi: 10.1177/0022034512444127
52. Zou W, Hunter N, Swain MV. Application of polychromatic μCT for mineral density determination. *J Dent Res* 2011; **90**: 18–30. doi: 10.1177/0022034510378429